American Journal of Pathology, Vol. 152, No. 1, January 1998

Temporal Pattern of Accelerated Lung Growth after Tracheal Occlusion in the Fetal Rabbit

Monique E. De Paepe,* Brian D. Johnson,† Konstantinos Papadakis,† Katsuo Sueishi,‡ and François I. Luks†

From the Department of Pathology and the Division of Pediatric Surgery,† Rhode Island Hospital and Brown University School of Medicine, Providence, Rhode Island, and the First Department of Pathology,‡ Kyushu University, Fukuoka, Japan*

Tracheal occlusion *in utero* is a potent stimulus of fetal lung growth. We describe the early growth mechanics of fetal lungs and type II pneumocytes after tracheal ligation (TL). Fetal rabbits underwent TL at 24 days gestational age (DGA; late pseudoglandular stage; term = 31 to 33 days) and were sacrificed at time intervals ranging from 1 to 5 days after TL. Lung growth was measured by stereological volumetry and bromodeoxyuridine (BrdU) pulse labeling. Pneumocyte II population kinetics were analyzed using a combination of anti-surfactant protein A and BrdU immunohistochemistry and computer-assisted morphometry. Nonoperated littermates served as controls. TL resulted in dramatically enhanced lung growth (lung weight/body weight was 5.00 ± 0.81% in TL *versus* 2.52 ± 0.13% in controls at 29 DGA; $P < 0.001$, unpaired Student's *t*-test). Post-TL lung growth was characterized by a 3-day lag-phase typified by relative stagnation of growth, followed by distension of airspaces, increased cell proliferation, and accelerated architectural and cellular maturation by postligation days 4 and 5. During the proliferation phase, the replicative activity of type II cells was markedly increased (type II cell BrdU labeling index was 10.0 ± 4.1% in TL *versus* 1.1 ± 0.3% for controls at 29 DGA; $P < 0.02$), but their numerical density decreased ($3.0 \pm 0.5 \times 10^{-3}/\mu m^2$ in TL *versus* $4.5 \pm 0.3 \times 10^{-3}/\mu m^2$ in controls at 29 DGA; $P < 0.02$), suggesting accelerated terminal differentiation to type I cells. In conclusion, post-TL lung development is characterized by a well defined temporal pattern of lung growth and maturation. The rabbit model lends itself well to study the regulatory mechanisms underlying accelerated fetal lung growth after TL. *(Am J Pathol 1998, 152:179–190)*

Tracheal occlusion is a potent *in vivo* model of accelerated fetal lung growth.[1–6] Animal experiments have shown that tracheal occlusion before birth can cause dramatic lung growth and maturation in fetuses with pulmonary hypoplasia.[7–9] Preliminary trials in humans have confirmed the potential usefulness of fetal tracheal obstruction in the antenatal treatment of congenital diaphragmatic hernia.[10,11] Little is known, however, about the underlying regulatory mechanisms of accelerated fetal lung growth. Knowledge of these cellular mechanisms may help elucidate the physiological and molecular basis of normal lung development and enable us to manipulate fetal and perinatal lung growth with, or even without, tracheal occlusion.

Previous studies of tracheal obstruction *in utero* have traditionally focused on fetal sheep and uniformly studied the late effects of prolonged occlusion (more than 1 week).[2,3,7,12] In contrast, the immediate and early effects (days) of tracheal ligation *in vivo* have not received much attention. The aim of the present study was to analyze the mechanics involved in the acceleration of fetal lung development with emphasis on the population kinetics and cytodifferentiation of type II pneumocytes. Type II pneumocytes are of great clinical relevance, as they produce pulmonary surfactant, serve as progenitors of the gas-exchanging type I pneumocytes, and are involved in ion transport in the alveolus.[13] Recent *in vitro* and *in vivo* studies have demonstrated quantitative and qualitative alterations in type II pneumocytes after prolonged fetal tracheal ligation.[12,14,15]

The fetal rabbit was selected as an animal model for this time course study. Aside from obvious attractive features of smaller laboratory animals such as low cost and large litter size, several attributes of rabbits make them particularly well suited for this type of study. The rabbit is probably the smallest mammal in which tracheal occlusion can be performed with acceptable survival rate.[1,4] The development of the fetal rabbit lung has been described in detail[16] and proceeds through the same stages as the human lung.[17] Unlike the advanced lung development of fetal sheep, which results in fully alveolarized lungs at term, less precocious rabbit, and human, lungs are only in the terminal air sac stage at term.

Tracheal ligation was performed at 24 days gestational age (DGA; late pseudoglandular stage). Lung development was studied at time intervals ranging from 1 to 5

Supported in part by research grant RG-159-N from the American Lung Association.

Accepted for publication October 2, 1997.

Address reprint requests to Dr. Monique E. De Paepe, Rhode Island Hospital, Department of Pathology, 593 Eddy Street, Providence RI 02903. E-mail: 103107.2777@compuserve.com.

days after tracheal ligation (25 to 29 DGA). Overall lung growth and the relative contributions of tissue and airspace compartments were evaluated by stereological volumetry. The population kinetics of type II pneumocytes were investigated by a combination of bromodeoxyuridine (BrdU) pulse labeling and computer-assisted morphometry, using anti-rabbit surfactant protein A (SP-A) antibodies for immunohistochemical identification of the cells. This antibody detects SP-A in alveolar type II cells and Clara cells early during fetal development[18] and is therefore suited for quantitation of fetal type II cells. Maturation and differentiation of type II pneumocytes were studied using ultrastructural criteria of type II cell differentiation.[16,19,20]

This study reveals that accelerated fetal lung growth after tracheal occlusion is characterized by a well coordinated time course of cell proliferation and maturation, suggesting the existence of strict regulatory cellular and molecular mechanisms.

Materials and Methods

Tracheal Ligation

Time-mated New Zealand White rabbits were obtained at 17 to 19 DGA (term = 31–33 days; Millbrook Farm, Amherst, MA). They were housed in separate cages under standard laboratory conditions, allowed free access to water and chow, and acclimated to their new environments. At 24 DGA, after a 12-hour fast, each doe was intramuscularly premedicated with xylazine (5 mg/kg) and ketamine (20 mg/kg). Cefazolin sodium (100 mg/kg) and medroxyprogesterone acetate (10 mg) were given at separate intramuscular sites. The abdomen was shaved. The rabbits were placed in supine position, intubated, and maintained under halothane anesthesia (1% to 3% in oxygen).

The gravid bicornuate uterus was exposed through a midline abdominal incision, and the ovarian-end fetuses were assigned to either tracheal ligation (TL) or control (C) groups. Tracheal ligation was limited to two alternate fetuses located at the ovarian end of the uterus. After fetal orientation was determined by gentle palpation, a purse-stringed antimesometrial hysterotomy was made over the fetal head using electrocautery to incise all layers of the uterine wall. The fetal head and neck were exposed, a midline cervical incision made, and the trachea identified. In TL fetuses, a mini hemoclip was placed across the trachea and the fetus returned to the amniotic cavity. Control fetuses consisted of sham-operated contralateral and adjacent littermates, who were manipulated through the wall of the exteriorized uterine horn. We refrained from sham hysterotomy on these fetuses to avoid oligohydramnios and its inherent risk of pulmonary hypoplasia.[4,8] The uterine wall was closed in one layer using a running, noninterlocking 5–0 polyglycolic acid suture (Vicryl, Ethicon, Johnson & Johnson, Cincinnati, OH). Maternal laparotomies were closed in two layers using 3–0 Vicryl (fascia) and 4–0 chromic (skin) sutures.

Animal Sacrifice and Tissue Processing

The animals were killed at time intervals ranging from 1 to 5 days after ligation (25 to 29 DGA). Two hours before death, the animals were weighed and intraperitoneally injected with 5′-bromo-2′-deoxyuridine (BrdU; Sigma Chemical Co., St. Louis, MO) dissolved in phosphate-buffered saline (PBS) at a dose of 50 mg/kg. The does were sacrificed (Beuthanasia-D Special, Shering-Plow Animal Health Corp., Kenilworth, NJ; 0.2 ml/kg, intracardiac). The midline incision was opened exposing the uterus, and fetuses were killed *in utero* by cardiac puncture before the first breath. All procedures and protocols were approved by the Rhode Island Hospital Animal Care and Use Committee.

Weights of fetus, lungs, liver, kidneys, and heart were recorded. The left lung was then weighed separately and immersion fixed *in toto* in freshly prepared 4% paraformaldehyde in PBS, pH 7.4. After overnight fixation at 21°C, the volume of the left lung was estimated by the volume displacement method.[21] The left lung was dehydrated in graded ethanol solutions and embedded in paraffin. Four-micron-thick sections were prepared and stained with hematoxylin and eosin (H&E) and periodic acid-Schiff (PAS; with diastase control) for glycogen. Samples from the right upper lobe were fixed in Karnovsky's fixative (4% paraformaldehyde, 2.5% glutaraldehyde, 0.1 mol/L sodium cacodylate buffer, pH 7.2) for ultrastructural analysis.

Radial Alveolar Count

As an index of alveolar proliferation, the radial alveolar count (RAC) as originally described by Emery and Mithal[22] was used. H&E-stained sections were examined at magnification ×40, and perpendicular lines were drawn from the lumen of respiratory bronchioles to the nearest connective tissue septum. The number of alveolar septa interrupted by this line was counted as an index of the development of the terminal respiratory unit.

Stereological Volumetry of Lungs

Morphometry of the various lung compartments was performed using standard stereological volumetric techniques.[23,24] H&E-stained tissue sections from the left lung were analyzed using a computerized image analysis system (Olympus BX-40 microscope (Olympus America, Melville, NY) interfaced via a CCD video camera (KP-161, Hitachi, Norcross, GA) to a Power Macintosh 7100/80AV (Apple Corp., Cupertino, CA) equipped with software for image analysis (Image NIH 1.59 for Macintosh, National Institutes of Health, Bethesda, MD). Data derived from measurements of the left lung were extrapolated to both lungs.

The critical data set and hierarchical equations, obtained by examining the lung at increasing levels of magnification, comprised the following:

1. Volume of lung: V(lu)

The volume of fixed lung was determined according to the Archimedes principle.[21] As the lungs of experimental and control animals were processed identically, no correction was made for dehydration and embedding.

2. Volume of parenchyma: $V(pa) = A_A(pa/lu) \times V(lu)$

Subsequent steps in the structural hierarchy involved point-counting methods based on computer-assisted image analysis. The number of fields to be examined for each type of measurement was determined by testing the reproducibility of results in a pilot study. The parenchymal areal density (A_A(pa/lu)) was estimated by dividing the number of points falling on parenchyma (lung excluding large-sized bronchi and blood vessels) by the number of points falling on the entire lung (magnification, ×10). The total parenchymal volume was calculated by multiplying A_A(pa/lu)by V(lu).

3. Volume of air-exchanging parenchyma:
$V(ae) = A_A(ae/pa) \times V(pa)$

The areal density of air-exchanging parenchyma (A_A(ae/pa) was estimated by studying random fields of peripheral lung parenchyma and dividing the number of points falling on air-exchanging parenchyma (peripheral lung parenchyma excluding airspace) by the number of points falling on the entire field (tissue and airspace; magnification, ×100). The total volume of air-exchanging parenchyma was calculated by multiplying A_A(ae/pa) by V(pa).

A_A(ae/pa) represents the tissue fraction of the lung and as such is the complement of the airspace fraction (ASF), a traditional measure of fetal lung maturation (A_A(ae/pa) = 1 − ASF).

Surfactant Immunohistochemistry and Type II Pneumocyte Morphometry

Sections of left lung were processed for avidin-biotin complex (ABC) immunoperoxidase staining[25] using a polyclonal anti-rabbit SP-A antiserum that reacts with type II cells and Clara cells.[18] After treatment with 3,3′-diaminobenzidine tetrachloride (Sigma), sections were lightly counterstained with hematoxylin, cleared, and mounted. Controls for specificity consisted of omission of the primary antibody.

Immunohistochemical anti-SP-A staining of type II and Clara cells produced a higher optical density than that of the background, allowing the SP-A-positive area to be evaluated automatically. The number of type II cells vastly outnumbered the number of Clara cells detected (type II cells accounted for 96 ± 4% of total SP-A-positive cells, as determined in a pilot study of samples from all experimental groups). The SP-A-positive area therefore closely reflects the type II pneumocyte area. For each section, the light intensity was standardized by threshold calibration using surfactant-negative interstitial tissue as standard. The SP-A-positive areal density (A_A(pnII/ae)), representing the SP-A immunoreactive area per unit area of air-exchanging parenchyma, was determined by dividing the points falling on SP-A-immunoreactive cells by the points falling on air-exchanging parenchyma (magnification, ×200). The type II pneumocyte cellular profile area (A(pnIIcell)) was measured manually by computer-assisted planimetry (magnification, ×600; at least 50 type II pneumocytes per animal from five different microscope fields). The numerical density of SP-A-positive cells (N_A(pnII/ae)), which reflects the number of type II cells, and Clara cells, per unit area of air-exchanging parenchyma, and the numerical density of SP-A-positive cells with reference to total cells (SP-A-positive cells/total number of cells) were measured automatically after threshold calibration (as above).

BrdU Immunohistochemistry

For immunohistochemical detection of BrdU-labeled nuclei, lung (and liver) sections were treated with H_2O_2, denatured in 2N HCl, washed in borate buffer (0.1 mol/L, pH 8.0), and incubated with monoclonal anti-BrdU antibody (Boehringer, Ingelheim, Germany). Bound antibody was detected using the ABC immunoperoxidase system[25] as above, followed by diaminobenzidine treatment and a light hematoxylin counterstain. The BrdU labeling of peripheral and central air-exchanging parenchyma was evaluated separately. Peripheral (subpleural) lung parenchyma was defined as air-exchanging parenchyma located within one ×40 high-power field of the pleura. The total number of nuclei in each of these compartments, and the number of BrdU-positive nuclei therein, were assessed semiautomatically using a computerized image analysis system. Results were expressed as the percentage of cells positive for BrdU (BrdU labeling index, BrdU-LI). For each animal, at least 5000 cells per air-exchanging zone were counted. Controls for specificity consisted of omission of the primary antibody.

Surfactant and BrdU Immunohistochemical Double Labeling

Double immunostaining for BrdU and surfactant was performed on sections denatured in 2N HCl, washed in borate buffer (0.1 mol/L, pH 8.0), and incubated with monoclonal anti-BrdU antibody (Boehringer), followed by detection using the ABC immunoperoxidase system[25] as above. After treatment with diaminobenzidine, the sections were incubated with polyclonal anti-rabbit SP-A antiserum. Bound anti-SP-A antibody was visualized using the ABC alkaline phosphatase system (Dako, Glostrup, Denmark) and naphthol-AS-MX-phosphate/fast red TR salt (NAMP/Fast Red, Sigma) as chromogen. To validate the results of the double-immunostaining procedure, sequential sections were independently stained for BrdU and SP-A using the same chromogens as in the double-staining procedure. The enzyme reactions yielded brown reaction products in the nucleus (BrdU) and red deposits in the cytoplasm (SP-A) that were easily distinguishable.

Table 1. Body Weight

	Body weight (g)				
	25 DGA	26 DGA	27 DGA	28 DGA	29 DGA
Control	15.7 ± 1.7 (7)	19.0 ± 3.7 (9)	21.9 ± 2.3 (9)	27.6 ± 8.4 (13)	33.5 ± 7.9 (14)
TL	14.2 ± 1.4 (4)	18.4 ± 1.7 (4)	21.4 ± 1.0 (3)	30.3 ± 5.3 (5)	32.5 ± 8.0 (3)

Values are expressed as mean ± SD of control and TL animals. Number of animals is shown in parentheses.

SP-A-positive and double BrdU- and SP-A-positive type II cells were counted manually (×400 magnification), and results were expressed as the percentage of type II pneumocytes positive for BrdU (Pn II BrdU-LI). At least 2000 type II cells were counted per lung.

Transmission Electron Microscopy

Tissue samples from the right upper lung lobe were fixed in Karnovsky's fixative, osmicated, dehydrated in ethanol, and embedded in epoxy resin. Ultrathin sections of blocks that did not contain large blood vessels or airways were stained with uranyl acetate and lead citrate and examined with a Philips 301 electron microscope operated at 60 kV.

Data Analysis

Statistical analysis was performed using the unpaired Student's *t*-test for comparison of control and experimental groups at each time point. A P value of <0.05 was considered statistically significant. Values are expressed as mean ± SD or, where appropriate, as mean ± SEM. Statview software (Abacus, Berkeley, CA) was used for all statistical work.

Results

Body and Organ Weights

The body weights of control and experimental fetuses were comparable at all time points, indicating that the surgical intervention was well tolerated (Table 1). Lung weight, normalized for body weight, was significantly greater in TL fetuses than in controls from post-ligation day 3 on and appeared to show a biphasic pattern characterized by a 15% increase on post-ligation days 3 and 4, followed by an abrupt additional 50% increase on post-ligation day 5 (Figure 1). The increase in organ weight was restricted to the lungs; the ratio of liver, kidney, and heart weight over body weight was the same for TL and control animals (not shown).

Histological Findings and Radial Alveolar Count

At 25 DGA, the lungs of control and TL fetuses were in the late pseudoglandular/early canalicular stage of development, characterized by glycogen-rich peripheral buds and rosettes showing various degrees of elongation and tortuosity (Figure 2a). On subsequent days, the lungs of control animals showed gradual architectural maturation to canalicular stage and, by 29 DGA, had all reached the terminal sac stage (Figure 2b). Prominent morphological changes of this period include depletion of cellular glycogen in type II cells (evidenced by loss of PAS positivity), thinning of the interstitium, rapid development of capillaries, and their angulation between alveolar epithelial cells.

From the third post-ligation day on, TL lungs showed accelerated distension of the airspaces and thinning of the alveolar septa, imparting the morphological impression of increased architectural maturity, when compared with controls. At 29 DGA, the alveolar septa of TL fetuses were thinner, red blood cells and capillaries were less prominent, and the airspaces less convoluted than in control animals, consistent with an early alveolar stage of development (Figure 2c). The morphological appearance of bronchial and vascular structures was comparable between the two groups.

The RAC of control lungs, a measure of architectural maturation of the terminal respiratory unit, showed a threefold increase between 25 and 29 DGA (Table 2). During the first 2 post-ligation days, the RAC of TL fetuses was similar to that of controls. From post-ligation day 3 on, the RAC of TL fetuses was significantly higher than that of controls, and it was almost twice as high on post-ligation day 5.

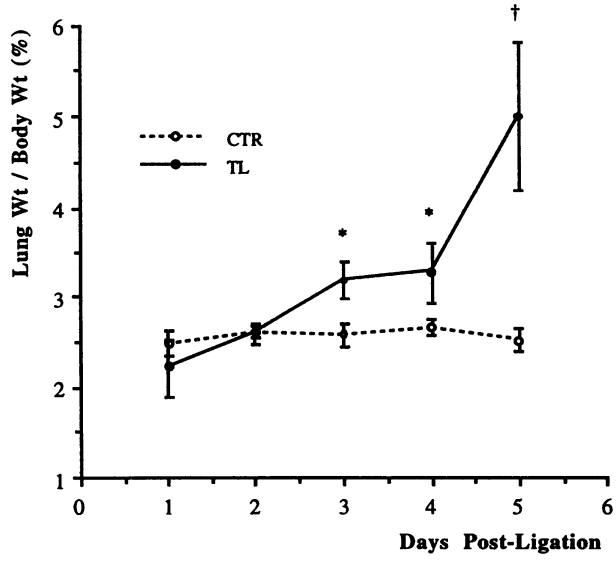

Figure 1. Lung weight/body weight. Values represent mean ± SD of control (CTR) and tracheal-ligated (TL) animals. $^{*}P < 0.05$, $^{\dagger}P < 0.01$ *versus* controls.

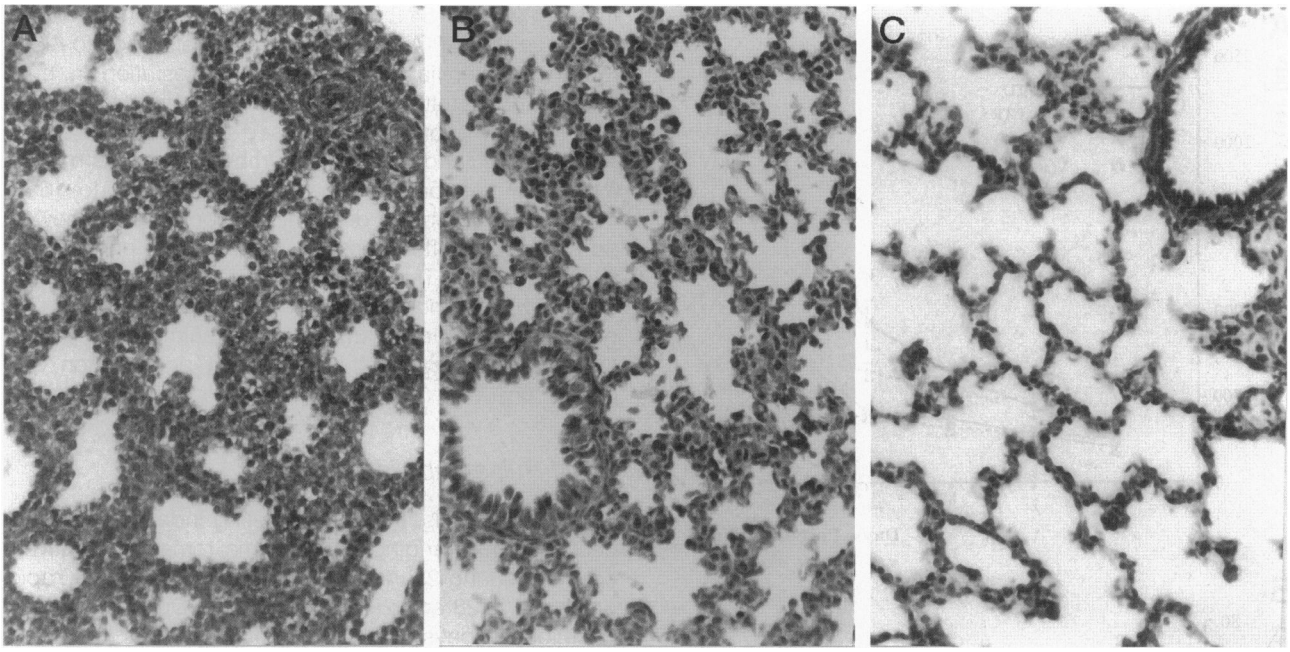

Figure 2. Light microscopic appearance of fetal lungs at 25 and 29 DGA. **a:** Control lungs at 25 DGA, late pseudoglandular stage, show thick and cellular alveolar septa lined by clear glycogen-rich epithelial cells. **b:** Control lungs at 29 DGA, terminal sac stage, show thinner but still cellular septa lined by a flattened epithelium. **c:** TL lungs at 29 DGA show attenuated and relatively acellular alveolar septa with crest formation, corresponding to early alveolar stage of development. H&E; original magnification, ×200.

Stereological Volumetry of the Lung

Between 25 and 29 DGA, the total lung volume (V(lu)) of TL fetuses showed a sixfold increase, significantly greater than the twofold increase of control fetuses (V(lu) = 1821 ± 478 μl in TL *versus* 769 ± 49 μl in controls at 29 DGA; $P < 0.01$). The areal density of lung parenchyma (A_A(pa/lu)), representing the peripheral parenchymal fraction not containing large-sized bronchi and vascular structures, ranged from 96 ± 2% to 99 ± 1% at the various time points and was always similar between control and TL fetuses. The total parenchymal volume (V(pa)), which is the product of V(lu) and A_A(pa/lu), therefore paralleled V(lu) and was significantly larger in TL fetuses after 4 days of ligation (Figure 3a).

The areal density of air-exchanging parenchyma (A_A(ae/pa)), representing the parenchymal tissue fraction, decreased at a faster rate in TL animals than in controls and, from post-ligation day 4 on, was significantly smaller in TL fetuses than controls (Figure 3b). The total volume of air-exchanging parenchyma (V(ae)), which takes into account both A_A(ae/pa) and V(pa), was nevertheless still similar in control and TL fetuses on post-ligation day 4 (Figure 3a), indicating that at this time point the V(pa) increase in TL fetuses is due to distension of airspaces rather than tissue increase. On post-ligation day 5, V(ae) was significantly greater in TL animals (Figure 3a), indicating absolute tissue growth, not merely lung distension. V(ae) expansion accounted for approximately 30% of the V(pa) increase between post-ligation days 4 and 5, the remainder being attributable to passive airspace distension (Figure 3a).

Surfactant Immunohistochemistry and Type II Pneumocyte Morphometry

SP-A immunoreactivity was first detected in rare scattered type II cells and Clara cells at 25 DGA and was consistently present in control and TL fetuses at 26 DGA. At approximately the same time, reaction product coated the lining of the alveolar walls. The lungs of TL animals at post-ligation days 4 and 5 appeared to have fewer SP-A-immunoreactive cells per area than control littermates (Figure 4, a and b). Intraluminal SP-A-positive secretions were seen from 26 to 27 DGA on, and were more prevalent in control animals than in TL animals (Figure 4, a and b).

Table 2. Radial Alveolar Count

	RAC (n)				
	25 DGA	26 DGA	27 DGA	28 DGA	29 DGA
Control	1.2 ± 0.0 (7)	1.9 ± 0.1 (9)	2.6 ± 0.2 (9)	2.9 ± 0.2 (13)	3.7 ± 0.2 (14)
TL	1.3 ± 0.2 (4)	2.1 ± 0.1 (4)	3.7 ± 0.4 (3)*	4.5 ± 0.3 (5)†	7.6 ± 0.5 (3)†

Values are expressed as mean ± SEM of control and TL animals.
*$P < 0.05$ *versus* controls.
†$P < 0.01$ *versus* controls.

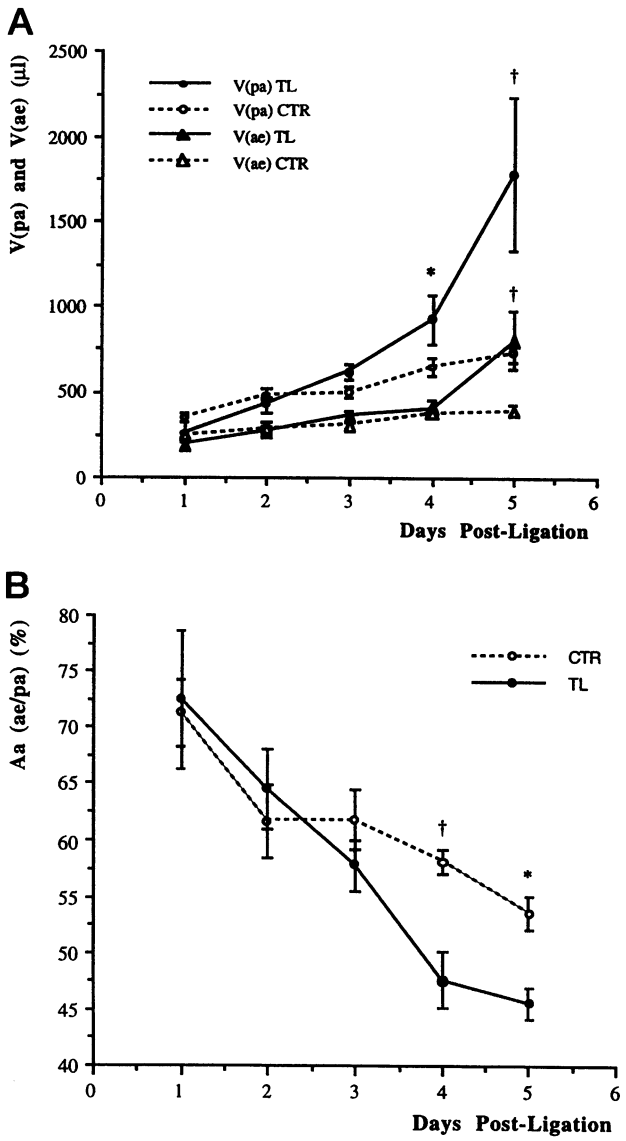

Figure 3. Stereological analysis. **a:** Total parenchymal volume (V(pa)) and air-exchanging parenchymal volume (V(ae)). **b:** Areal density of air-exchanging parenchyma (A_A(ae/pa)). Values represent mean ± SEM of control (CTR) and tracheal-ligated (TL) animals. See Table 1 for number of animals studied. $^*P < 0.05$, $^\dagger P < 0.01$ *versus* controls.

Morphometry of SP-A-positive cells was restricted to post-ligation days 2 through 5 (26 to 29 DGA). In controls, the SP-A-positive areal density (A_A(pnII/ae)) showed a more than twofold increase during this time period (Figure 5a). In TL fetuses, A_A(pnII/ae) also increased initially, although to lower values than controls. On post-ligation day 5, a dramatic decrease in A_A(pnII/ae) was observed in TL animals, to only one-half the value of control animals (8.17 ± 0.38% in controls *versus* 4.43 ± 0.09% in TL; $P < 0.01$; Figure 5a). The average cellular profile area of type II pneumocytes (A(pnIIcell)) decreased with gestation in control animals (57.5 ± 2.8 μm^2 at 25 DGA *versus* 43.9 ± 1.9 μm^2 at 29 DGA). The cellular profile area of TL animals was initially smaller than controls (44.1 ± 2.1 μm^2 at 25 DGA; $P < 0.01$) but progressively increased with gestation, and was significantly larger than that of controls at 29 DGA (54.3 ± 0.7 μm^2; $P < 0.05$). The numerical density of SP-A-positive cells with reference to A(ae) (N_A(pnII/ae)) initially increased with gestation in both control and TL fetuses. Between post-ligation days 4 and 5, N_A(pnII/ae) abruptly decreased by 20% (Figure 5b). The total cellular density (total number of cells per mm^2 of air-exchanging parenchyma) ranged from 12 to 16 × $10^3/mm^2$ between the different time points and showed no significant differences between control and experimental animals. The numerical density of SP-A-positive cells with reference to total cell number increased with gestation in controls but, in ligated animals, showed a significant decrease after the fourth post-ligation day (Figure 5c).

BrdU Pulse Labeling

In control animals, the BrdU labeling index (BrdU-LI) of central air-exchanging parenchyma remained relatively constant during 25 through 27 DGA, followed by a rapid decrease at 28 and 29 DGA (Table 3). During the first 2 post-ligation days, the BrdU-LI of TL fetuses paralleled that of control fetuses. On post-ligation day 3 (27 DGA), the proliferative rate of TL lungs showed a significant suppression compared with that of controls, only to show a proliferative surge 1 and 2 days later (Table 3). In controls, most proliferative activity was seen in the interstitium whereas TL lungs showed many BrdU-labeled nuclei along the epithelial aspect of the alveolar septa (Figure 6).

The peripheral (subpleural) air-exchanging parenchyma showed an overall higher proliferative rate than the central parenchyma, with the same temporal pattern of alterations, including initial depression, followed by significantly increased proliferation in TL animals (Table 3).

To determine whether these alterations in proliferation were restricted to the lung, the BrdU-LI of liver cells was determined. No difference in liver cell proliferation was found between control and TL animals at any time point (not shown).

BrdU-SP-A Double Labeling

To investigate whether the decreased numerical density of type II pneumocytes observed after 4 days of tracheal ligation could be ascribed to decreased cell proliferation, the BrdU-LI of SP-A-positive cells was determined. In control animals, the BrdU-LI of SP-A-immunoreactive type II cells rapidly decreased between 27 and 29 DGA. In TL fetuses, on the other hand, the proliferative activity of type II cells was found to increase dramatically at this time, with a peak at post-ligation day 4 (Figure 7). At 29 DGA, the BrdU-LI of SP-A-positive type II pneumocytes was more than fourfold higher in TL fetuses than in control fetuses (Figures 7 and 8).

Transmission Electron Microscopy

At 25 DGA, the ultrastructural features of lung were similar in fetal control and TL animals. In both groups, the

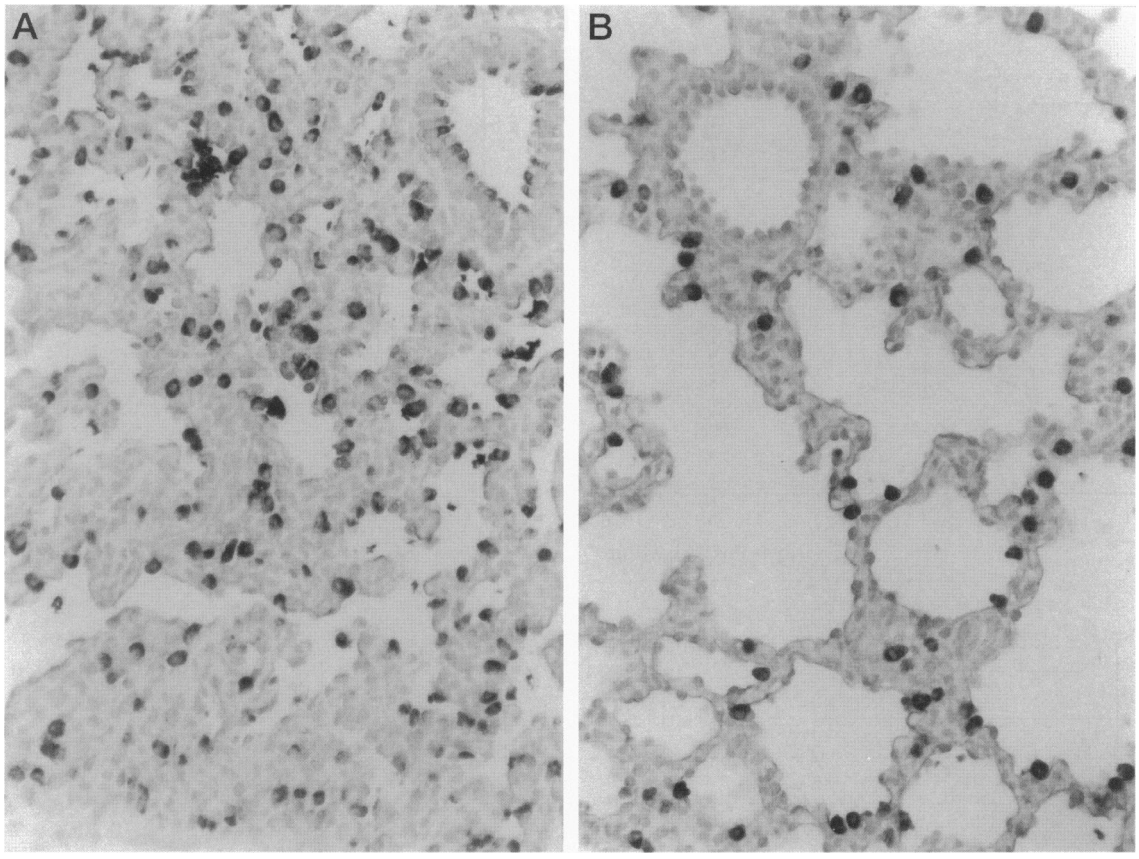

Figure 4. Surfactant protein A-immunohistochemical staining of fetal lungs at 28 DGA. **a:** Control lungs at 28 DGA show numerous dark-stained type II cells lining the alveolar septa. Immunoreactive Clara cells are seen in the respiratory bronchiole. **b:** The type II cells of TL lungs appear less abundant and larger in size. SP-A immunostaining by ABC-method, hematoxylin counterstain; original magnification, ×200.

alveolar septa were thick and cellular. Type II pneumocytes, recognizable by their cuboidal shape, microvillous projections, and occasional presence of dense, multivesicular, or immature lamellar bodies, were equally undifferentiated in both groups. The cytoplasm was filled with glycogen (washed out with the preparation method used) and contained few organelles, mostly mitochondria and Golgi complexes. At 26 DGA, the majority of type II cells of control fetuses still contained large amounts of cytoplasmic glycogen pools with relatively few multivesicular and immature lamellar bodies (Figure 9a). In TL fetuses, in contrast, most type II cells showed depletion of cellular glycogen stores in association with increased abundance and enhanced maturity of lamellar bodies (Figure 9b). At this stage of development, the alveoli of TL fetal lungs contained small intra-alveolar tubular myelin and secreted lamellar bodies, whereas these were not seen in control lungs.

With progressing gestational age, the lungs showed more advanced ultrastructural evidence of cytodifferentiation. The alveolar wall was thicker in control than TL fetuses and contained more centrally placed capillaries. The type II cells of TL fetuses showed higher lamellar body content. The number of intra-alveolar inclusions at 28 DGA was higher in control than in TL fetuses. At 28 DGA, glycogen deposits were virtually absent in both experimental groups.

Discussion

The present study is the first to document the early temporal sequence of lung and type II cell growth after *in utero* tracheal occlusion. Tracheal ligation was performed in fetal rabbits at day 24 of their 31-day gestation. At this time point, rabbit lungs are in the late pseudoglandular stage, corresponding to a gestational age of 16 weeks in humans and 110 days in sheep. Our results demonstrate that the early lung growth after tracheal occlusion is characterized by a coordinated temporal sequence of cellular events. The first 3 post-ligation days are typified by a relative stagnation of lung growth. During this lag phase, total parenchymal volume (V(pa)), as well as total air-exchanging parenchymal volume (V(ae)), which represents the parenchymal tissue compartment, do not differ between controls and TL fetuses. Similarly, the proliferative rates of TL lungs are the same, or even lower, than those of controls. The decreased lung growth in the first 3 post-ligation days parallels the significant fall in lung fluid production noted in the first post-ligation days in the fetal lamb model.[6]

The initial lag period is followed by a period of dramatic lung growth, attributed to both distension and cell proliferation. At post-ligation day 4, V(pa) was found to be significantly higher in TL animals than controls, whereas at this time the volume of the tissue compartment (V(ae))

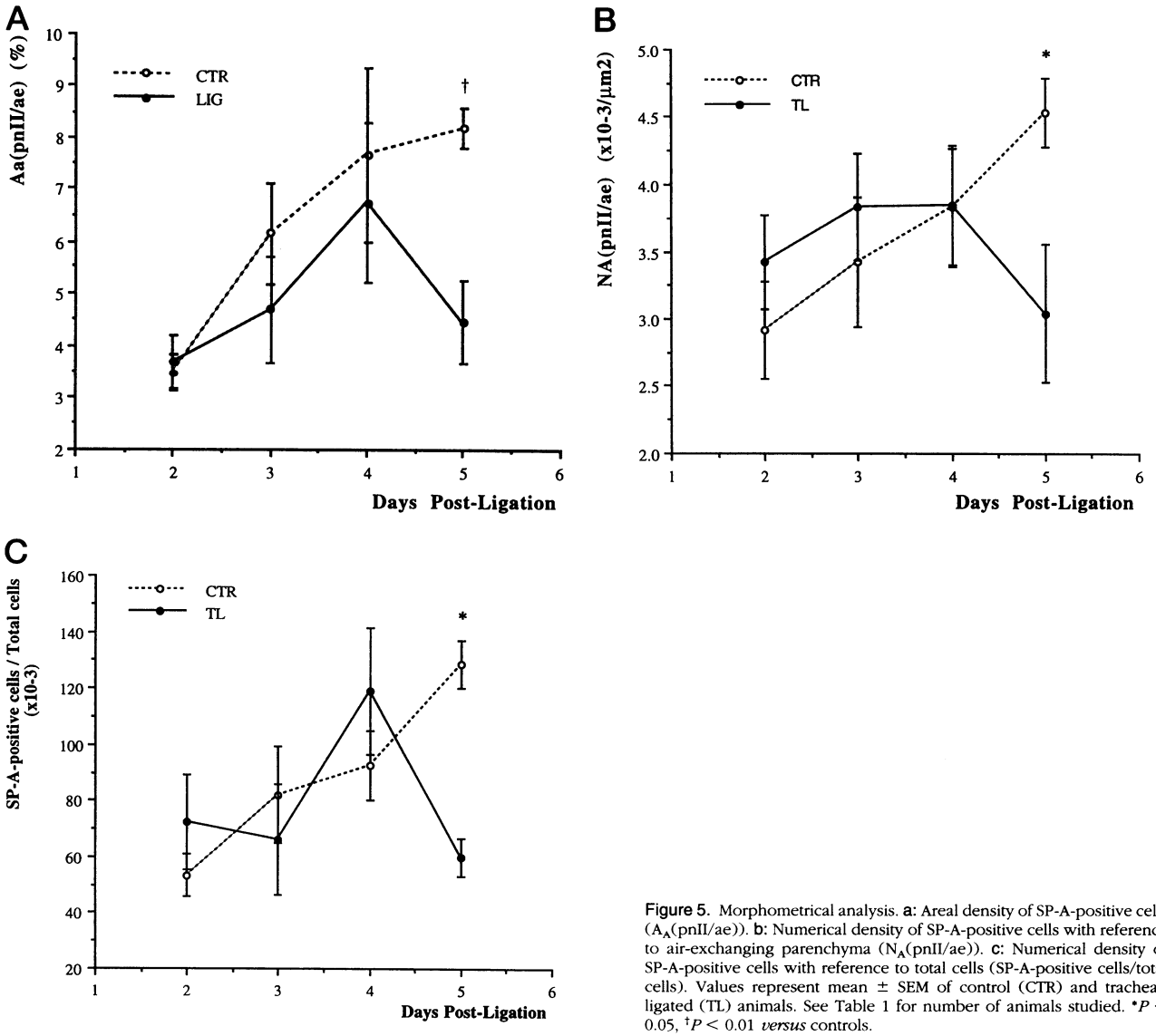

Figure 5. Morphometrical analysis. **a:** Areal density of SP-A-positive cells (A_A(pnII/ae)). **b:** Numerical density of SP-A-positive cells with reference to air-exchanging parenchyma (N_A(pnII/ae)). **c:** Numerical density of SP-A-positive cells with reference to total cells (SP-A-positive cells/total cells). Values represent mean ± SEM of control (CTR) and tracheal-ligated (TL) animals. See Table 1 for number of animals studied. $^*P < 0.05$, $^\dagger P < 0.01$ *versus* controls.

was not significantly increased. The *V*(pa) increase with unchanged *V*(ae) indicates that the initial lung growth is due to passive distension of the airspaces rather than actual tissue growth. The brief distension phase at day 4 was followed by additional increase of *V*(pa) at day 5, which was accompanied by an increase of *V*(ae), reflecting that the increased total parenchymal volume is due to expansion of both airspace and tissue compartments of the peripheral lung parenchyma. Even at this time point, the distension of pre-existing airspaces predominates: the additional increase in *V*(lu) between days 4 and 5 is approximately 70% due to distension and 30% due to tissue growth. The distension of TL lungs was associated with a dramatic increase in cell proliferation from

Table 3. BrdU Labeling Index (%)

	BrDU-LI (%)				
	25 DGA	26 DGA	27 DGA	28 DGA	29 DGA
Center					
Control	10.5 ± 1.3 (7)	8.5 ± 1.7 (9)	10.6 ± 0.7 (9)	4.4 ± 0.7 (13)	2.7 ± 0.5 (14)
TL	10.5 ± 4.4 (4)	5.9 ± 3.1 (4)	6.2 ± 2.1 (3)*	7.3 ± 0.8 (5)*	10.1 ± 0.6 (3)†
Periphery					
Control	17.7 ± 2.2	14.2 ± 3.8	15.8 ± 1.2	9.0 ± 1.7	6.2 ± 1.0
TL	16.7 ± 6.0	10.1 ± 3.8	10.5 ± 2.3*	16.0 ± 1.6*	16.7 ± 2.8†

Values are expressed as mean ± SEM of control and TL animals. Number of animals is shown in parentheses.
*$P < 0.05$ *versus* controls.
†$P < 0.001$ *versus* controls.

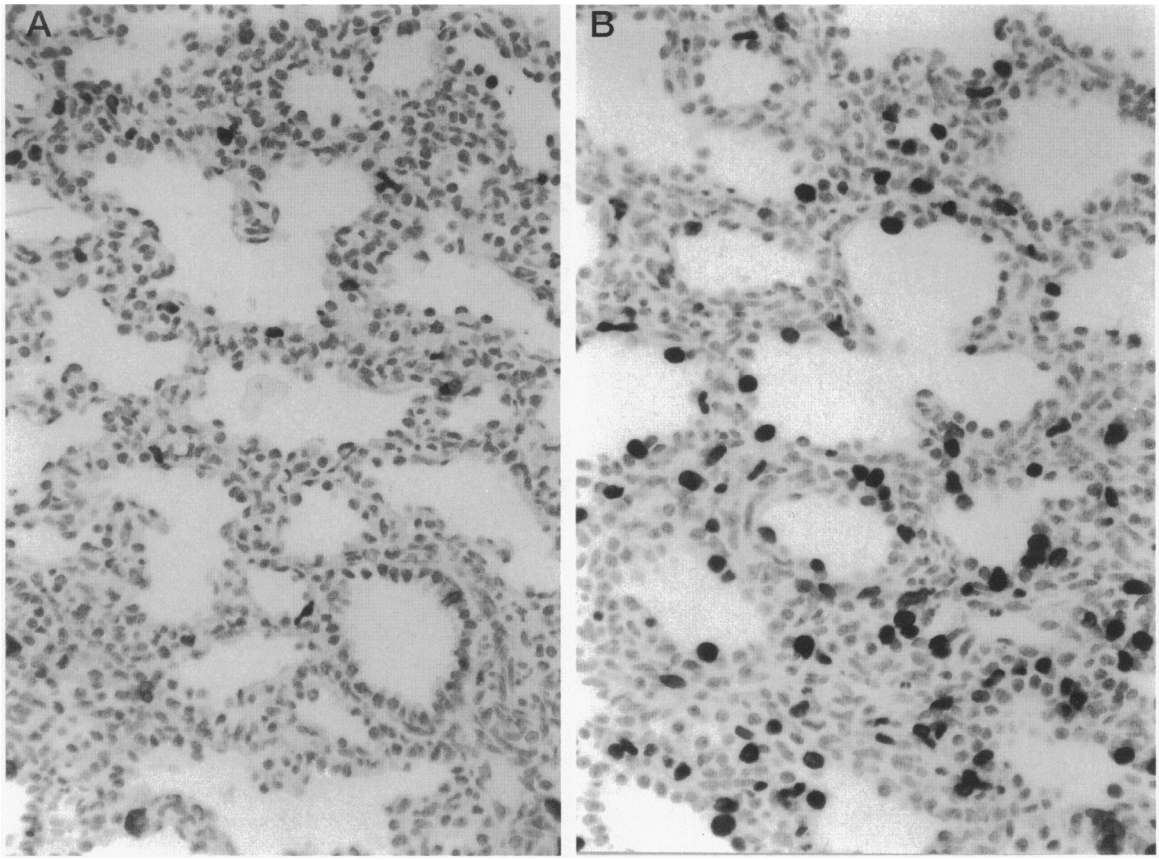

Figure 6. BrdU labeling of fetal lungs at 28 DGA. **a:** Control lungs at 28 DGA show relatively little proliferative activity, which is mostly present within the interstitium. **b:** TL lungs at 28 DGA show more BrdU-labeled nuclei, located both in interstitium and along the epithelial aspect of the septa. BrdU labeling by modified ABC method, hematoxylin counterstain; original magnification, ×200.

post-ligation day 4 on, further confirming net cellular growth.

The lung growth induced by TL is associated with accelerated architectural maturation, as defined in this study by more advanced developmental stage and higher radial alveolar count (RAC).[22] This finding is in concordance with observations in sheep, where others have described increased alveolar number and increased RAC after TL.[26]

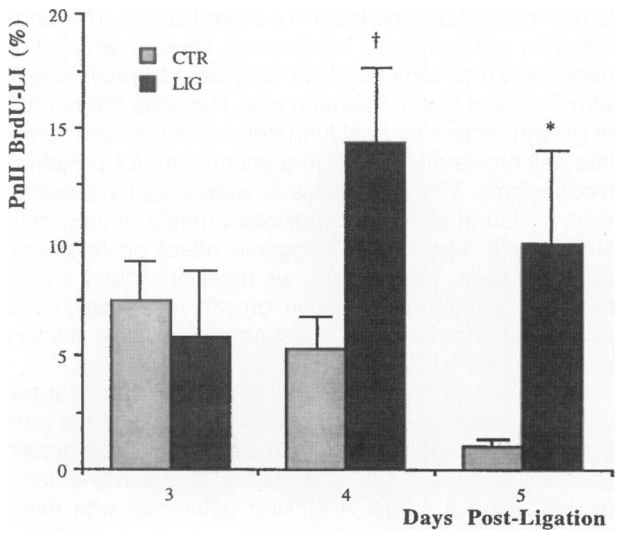

Figure 7. BrdU labeling of type II cells. Values represent mean ± SEM of control (CTR) and tracheal-ligated (TL) animals. See Table 1 for number of animals studied. $^{*}P < 0.05$, $^{\dagger}P < 0.01$ *versus* controls.

In addition to overall lung maturation, cellular differentiation of type II cells was evaluated ultrastructurally, based on the observation that, with increasing maturity, type II pneumocytes show decreased glycogen and increased lamellar and multivesicular body content.[16,20,27] Whereas the ultrastructural development of control lungs followed the expected pattern, the lungs of TL fetuses showed ultrastructural evidence of accelerated type II pneumocyte maturation, consisting of early disappearance of glycogen concomitant with the presence of mature lamellar bodies. Accelerated type II cytodifferentiation of TL lungs was seen as early as post-ligation day 2, before the observation of alterations by light microscopy.

Computer-assisted morphometry combined with anti-surfactant protein immunohistochemistry allowed us to specifically evaluate the type II cell compartment during the post-ligation lung growth spurt. Whereas initially type II cells of ligated lungs tended to be slightly more numerous, and smaller, than those of controls, later the numerical density of type II cells was much lower in ligated lungs. The relative reduction of the type II pneumocyte population in all likelihood heralds the onset of the severe type II cell depletion observed after more prolonged TL in

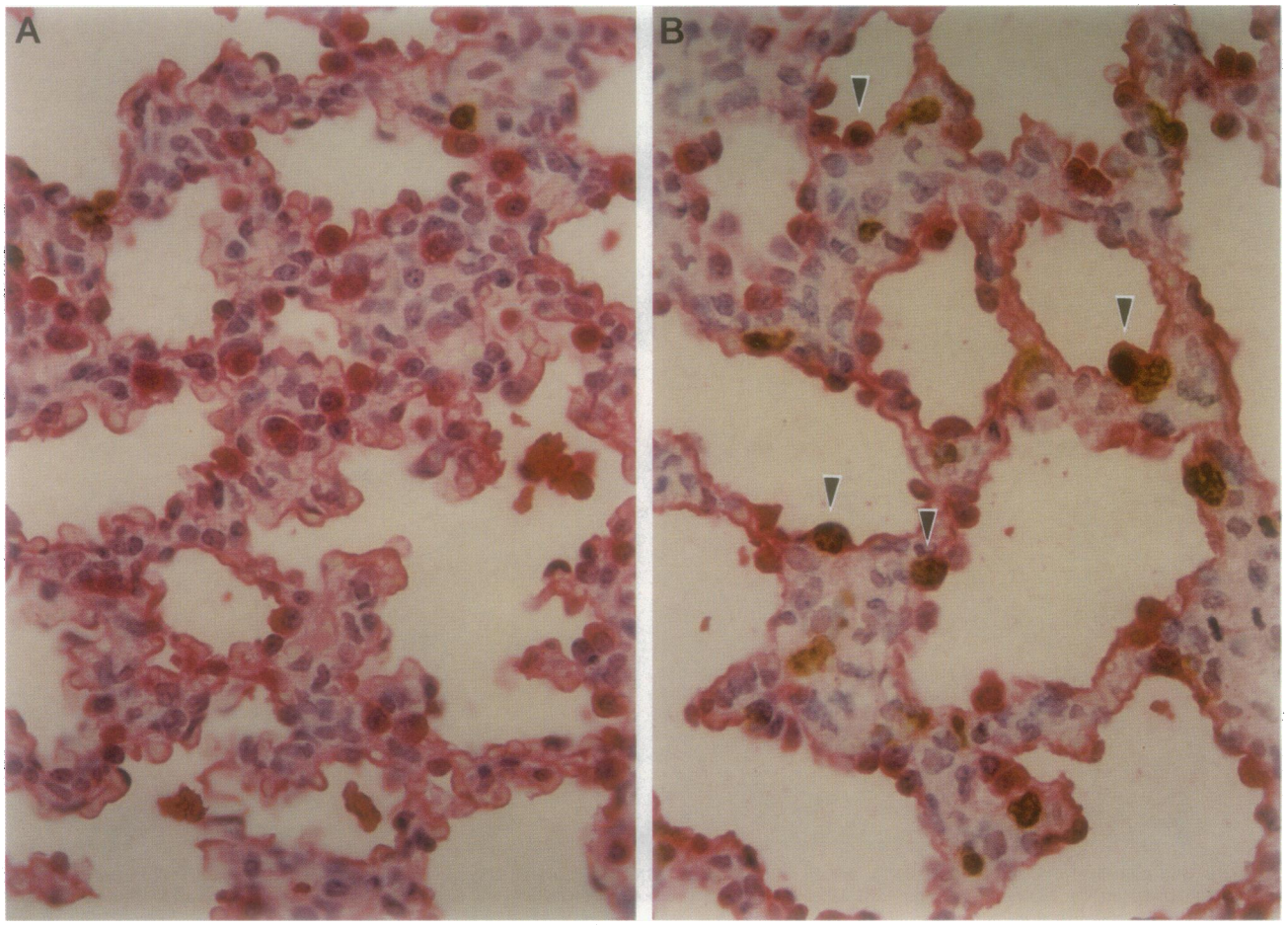

Figure 8. BrdU and SP-A double labeling of fetal lungs at 28 DGA. **a:** Control lungs at 28 DGA show numerous type II cells (red cytoplasm). BrdU-labeled nuclei (brown) are mainly seen in the interstitium. **b:** TL lungs at 28 DGA show proliferative activity in a large proportion of type II cells (**arrowheads**). BrdU and SP-A labeling by modified ABC method, hematoxylin counterstain; original magnification, ×400.

sheep.[12,14] It is uncertain what causes the reduction of the type II cell population. In theory, the decrease of type II cells could be attributed to three mechanisms, possibly acting together: decreased type II cell proliferation, increased type II cell death, or increased differentiation to type I cells. By combining BrdU pulse labeling with SP-A immunohistochemistry, the proliferative rate of type II cells could be monitored over the post-ligation course. Rather than being diminished, the BrdU-LI index of type II cells was found to be paradoxically higher on post-ligation day 4, coinciding with the onset of their rapid decline. Although the samples were not tested for the presence of apoptotic cells, there was no morphological evidence of cell death (necrosis or apoptosis) in this study. It is therefore tempting to postulate that the observed type II cell reduction is in large part attributable to accelerated terminal differentiation of these cells to type I pneumocytes.

The extent of lung growth induced by intrauterine tracheal occlusion is dramatic; the lung weight/body weight ratio was found to be doubled in 5 days. Although this phenomenon has been recognized for more than 20 years,[1,2] the mechanism of post-ligation lung growth remains uncertain. Both mechanotransduction (stretch) and local effects of growth factors have been implicated, probably acting in concert.[6] Tracheal ligation results in increased intratracheal pressure,[6,26,28] presumably due to continuous fluid secretion in a closed space. The lungs are thus subjected to mechanical stretch, which has been shown to stimulate fetal lung cells to proliferate *in vitro*[29–31] and *in vivo*.[5] Stretch may stimulate the release of growth factors by fetal lung cells, which in turn stimulate cell proliferation through autocrine and/or paracrine mechanisms. This hypothesis is supported by observations by Liu et al[31] that conditioned media of lung cells stretched *in vitro* has a mitogenic effect on fetal lung epithelial cells. Furthermore, we have previously shown that the post-tracheal ligation growth response *in vivo* partly depends on the presence of soluble factors present in the tracheal fluid.[6]

The well defined time course of lung growth after tracheal occlusion *in utero* imitates to some extent the temporal pattern described during the early postnatal growth spurt of the newborn and the post-pneumonectomy growth of adult lungs. A striking difference with these examples of rapid lung growth is the presence of a 3-day lag period between tracheal occlusion and increased lung growth. Indeed, both in post-pneumonectomy com-

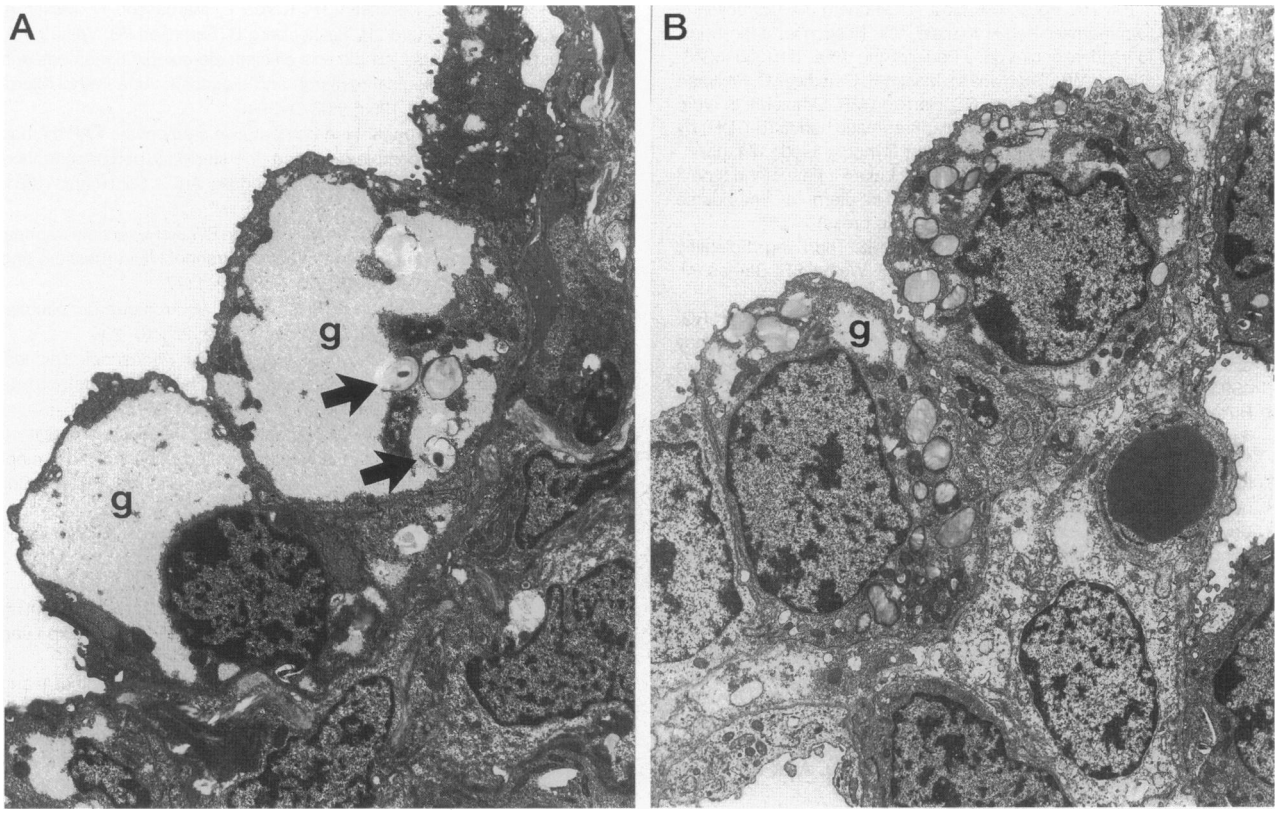

Figure 9. Ultrastructural appearance of fetal lungs at 26 DGA. **a:** Type II pneumocytes from control rabbit fetus at 26 DGA. Type II cells are recognized by their cuboidal shape and the presence of immature lamellar bodies (**arrows**). Extensive glycogen (g) lakes (partially washed out) fill the cytoplasm. **b:** Type II pneumocytes from TL rabbit fetus at 26 DGA (post-ligation day 2). Numerous large and mature lamellar bodies are seen. Small residual glycogen deposits (g) are scattered between the lamellar bodies. Uranyl acetate, lead citrate; final magnification, ×6600).

pensatory lung growth and early postnatal lung growth, the lung response is almost immediate, and characterized by initial expansion by overinflation, followed after 2 to 4 days by an increase in tissue mass and cell proliferation.[32–35] Whether the 3-day lag period is related to the presence of local growth-inhibitory factors in the tracheal fluid, or to the immaturity of the lungs, remains to be elucidated. However, local inhibitory factors are not likely implicated, as we have shown in the lamb model that TL lungs display the same lag phase, and less growth, when tracheal fluid is replaced by a normal saline solution.[6]

In summary, this study documents the coordinated temporal pattern of lung growth and type II cell proliferation after intrauterine TL in rabbits. Knowledge of this time course may have immediate clinical implications with regard to timing and duration of fetal intervention in pulmonary hypoplasia disorders. Type II cells are induced to proliferate within a specific time frame, which may be of critical importance in the timing of gene therapy for genetically determined disorders such as SP-B deficiency and cystic fibrosis where type II cells are the transfection target cells. The existence of a coordinated time course of post-TL growth suggests tight regulation by cellular/molecular mechanisms that integrate mechanotransduction (stretch) and hormonal stimuli and mediate epithelial-mesenchymal interactions in the maturing lung.

References

1. Carmel JA, Friedman F, Adams FH: Fetal tracheal ligation and lung development. Am J Dis Child 1965, 109:452–456
2. Alcorn D, Adamson TM, Lambert TF, Maloney JE, Ritchie BC, Robinson PM: Morphological effects of chronic tracheal ligation and drainage in the fetal lamb lung. J Anat 1977, 123:649–660
3. Lanman JT, Schaffer A, Herod L, Ogawa Y, Castellanos R: Distensibility of the fetal lung with fluid in sheep. Pediatr Res 1971, 5:586–590
4. Adzick NS, Harrison MR, Glick PL, Villa RL, Finkbeiner W: Experimental pulmonary hypoplasia and oligohydramnios: relative contributions of lung fluid and fetal breathing movements. J Pediatr Surg 1984, 19:658–665
5. Hooper SB, Han VKM, Harding R: Changes in lung expansion alter pulmonary DNA synthesis and IGF-II gene expression in fetal sheep. Am J Physiol 1993, 265:L403–409
6. Papadakis K, Luks FI, De Paepe ME, Piasecki GJ, Wesselhoeft CW Jr: Fetal lung growth after tracheal ligation is not solely a pressure phenomenon. J Pediatr Surg 1997, 32:347–351
7. DiFiore JW, Fauza DO, Slavin R, Peters CA, Fackler JC, Wilson JM: Experimental fetal tracheal ligation reverses the structural and physiological effects of pulmonary hypoplasia in congenital diaphragmatic hernia. J Pediatr Surg 1994, 29:248–257
8. Hedrick MH, Estes JM, Sullivan KM, Bealer JF, Kitterman JA, Flake AW, Adzick NS, Harrison MR: Plug the lung until it grows (PLUG): A new method to treat congenital diaphragmatic hernia in utero. J Pediatr Surg 1994, 29:612–617
9. Nardo L, Hooper SB, Harding R: Lung hypoplasia can be reversed by short-term obstruction of the trachea in fetal sheep. Pediatr Res 1995, 38:690–696
10. Harrison MR, Adzick NS, Flake AW, Vanderwall KJ, Beaker JF, Howell

LJ, Farrell JA, Filly RA, Rosen MA, Sola A, Goldberg JD: Correction of congenital diaphragmatic hernia in utero. VIII. Response of the hypoplastic lung to tracheal occlusion. J Pediatr Surg 1996, 31:1339–1348
11. Flake AW, Johnson MP, Treadwell M, Mason B, Cauldwell C, Phillipart AI, Cullen ML, O'Brien J, Adzick NS, Harrison MR, Evans MI: In utero treatment of right-sided congenital diaphragmatic hernia (R-CDH) by prenatal tracheal occlusion. Am J Obstet Gynecol 1996, 174:489
12. De Paepe ME, Papadakis K, Johnson BD, Luks FI: Fate of the type II pneumocyte following tracheal occlusion in utero: a time-course study in fetal sheep. Virchows Arch 1997 (in press)
13. Mason RJ, Shannon JM: Alveolar type II cells. The Lung: Scientific Foundations. Edited by Crystal RG, West JB, Weibel ER, Barnes PJ. Philadelphia, Lippincott-Raven, 1997, pp 534–555
14. O'Toole SJ, Sharma A, Karamanoukian HL, Holm B, Azizkhan RG, Glick PL: Tracheal ligation does not correct the surfactant deficiency associated with congenital diaphragmatic hernia. J Pediatr Surg 1996, 31:546–550
15. Bullard KM, Sonne J, Hawgood S, Harrison MR, Adzick NS: Tracheal ligation increases cell proliferation but decreases surfactant protein in fetal murine lungs in vitro. J Pediatr Surg 1997, 32:207–213
16. Kikkawa Y, Motoyama EK, Gluck L: Study of the lungs of fetal and newborn rabbits: morphologic, biochemical and surface physical development. Am J Pathol 1968, 52:177–210
17. Pringle KC: Human fetal lung development and related animal models. Clin Obstet Gynecol 1986, 29:502–513
18. Asabe K, Toki N, Hashimoto S, Suita S, Sueishi K: An immunohistochemical study of the expression of surfactant apoprotein in the hypoplastic lung of rabbit fetuses induced by oligohydramnios. Am J Pathol 1994, 145:631–639
19. Williams MC, Mason RJ: Development of the type II cells in the fetal rat lung. Fed Proc 1977, 12:37–47
20. Snyder JM, Magliato SA: An ultrastructural, morphometric analysis of rabbit fetal lung type II cell differentiation in vivo. Anat Rec 1991, 229:73–85
21. Aherne WA, Dunnill MS: The estimation of whole organ volume. Morphometry. Edited by Aherne WA, Dunnill MS. London, Edward Arnold, 1982, pp 10–18
22. Cooney TP, Thurlbeck WM: The radial alveolar count method of Emery and Mithal: a reappraisal. I. Postnatal lung growth. Thorax 1982, 37:572–579
23. Bolender RP, Hyde DM, Dehoff RT: Lung morphometry: a new generation of tools and experiments for organ, tissue, cell, and molecular biology. Am J Physiol 1993, 265:L521–L548
24. Gundersen HJG, Bendtsen TF, Korbo L, Marcussen N, Møller A, Nielsen K, Nyengaard JR, Pakkenberg B, Sørensen FB, Vesterby A, West MJ: Some new, simple and efficient stereological methods and their use in pathological research and diagnosis. Acta Pathol Microbiol Immunol Scand 1988, 96:379–394
25. Hsu SM, Raine L, Fanger H: A comparative study of the PAP method and avidin-biotin complex method for studying polypeptide hormones with radioimmunoassay antibodies. Am J Clin Pathol 1981, 75:734–738
26. Hashim E, Laberge J-M, Chen M-F, Quillen EW Jr: Reversible tracheal obstruction in the fetal sheep: effects on tracheal fluid pressure and lung growth. J Pediatr Surg 1995, 30:1172–1177
27. Reid L, Meyrick B: Etude au microscope électronique du poumon foetal de lapin: le poumon et le coeur. 1969, 25:210–206
28. Luks I, Gilchrist BF, Jackson BT, Piasecki GJ: Endoscopic tracheal obstruction with an expanding device in a fetal lamb model: preliminary considerations. Fetal Diagn Ther 1996, 11:67–71
29. Scott JE, Yang S-Y, Stanik E, Anderson JE: Influence of strain on [^{3}H]thymidine incorporation, surfactant-related phospholipid synthesis, and cAMP levels in fetal type II alveolar cells. Am J Respir Cell Mol Biol 1993, 8:258–265
30. Liu M, Skinner SJM, Xu J, Han RNN, Tanswell AK, Post M: Stimulation of fetal rat lung cell proliferation in vitro by mechanical stretch. Am J Physiol 1992, 263:1376–1383
31. Liu M, Xu J, Tanswell K, Post M: Stretch-induced growth-promoting activities stimulate fetal rat lung epithelial cell proliferation. Exp Lung Res 1993, 19:505–517
32. Romanova LK, Leikina EM, Antipova KK: Nucleic acid synthesis and mitotic activity during development of compensatory hypertrophy of the lung in rats. Bull Exp Biol Med 1967, 63:303–306
33. Brody JS, Burki R, Kaplan N: Deoxyribonucleic acid synthesis in lung cells during compensatory lung growth after pneumonectomy. Am Rev Respir Dis 1978, 117:307–316
34. Rannels DE, White DM, Watkins CA: Rapidity of compensatory lung growth following pneumonectomy in adult rats. J Appl Physiol 1979, 46:326–333
35. Berger LC, Burri PH: Timing of the quantitative recovery in the regenerating rat lung. Am Rev Respir Dis 1985, 132:777–783
36. Simnett J, Fisher JM, Heppelston AG: Tissue-specific inhibition of lung alveolar cell mitosis in organ culture. Nature 1969, 223:944–946